A novel approach to automatic position calibration for pixelated crystals in gamma imaging

Original Article

Salar Sajedi[1], Navid Zeraatkar[2], Sanaz Kaviani[1], Hadi Khanmohammadi[1], Saeed Sarkar[3], Hamid Sabet[4], Mohammad Reza Ay[1,5]

[1]Research Center for Molecular and Cellular Imaging, Tehran University of Medical Sciences, Tehran, Iran
[2]Department of Radiology, University of Massachusetts Medical School, Worcester, MA, USA
[3]Research Center for Science and Technology in Medicine, Tehran University of Medical Sciences, Tehran, Iran
[4]Department of Radiology, Massachusetts General Hospital, Harvard Medical School, Boston, USA
[5]Department of Medical Physics and Biomedical Engineering, Tehran University of Medical Sciences, Tehran, Iran

(Received 27 November 2018, Revised 14 January 2019, Accepted 16 January 2019)

ABSTRACT

Introduction: The position estimation in gamma detection system will have constant misplacements which can be corrected in the calibration procedure. In the pixelated crystal uniformly irradiation of detector will produce irregular shape due to position estimation errors. This image is called flood field image and is used to calibrate the position estimation. In this work we present a novel approach to automatically calibrate pixelated crystal array position estimation.

Methods: In the flood image of a pixelated crystal array the local peaks represent the estimation of position for the gamma photons that interacted in a single crystal pixel. First, the method detects 2-D peak locations automatically in the case of blurred pixel responses in the presence of noise and disturbance of the image. The algorithm consists of a filtering step for smoothing the image followed by two rounds of local peak detection. After localizing image peaks, the correction routine will map the image locations to the crystal pixels using the thin-plate spline interpolation method.

Results: The algorithm is tested for two flood images obtained from developed detector with different irregularity levels. By configuring constant parameters according to the detector configuration the method detected all crystal pixels in the image and map them correctly. The method further has been tested for10 identical blocks and the result showed automatic peak detection routine for all the blocks.

Conclusion: An automatic peak detection is presented to work instead of time consuming manual calibration routines. The method shows robust performance in the presence of image noise.

Key words: Positron emission tomography; Position calibration; Pixelated crystal; Gamma detector

Iran J Nucl Med 2019;27(2):106-112
Published: July, 2019
http://irjnm.tums.ac.ir

Corresponding author: Mohammad Reza Ay, Department of Medical Physics and Biomedical Engineering, Tehran University of Medical Sciences, Tehran, Iran. E-mail: mohammadreza_ay@sina.tums.ac.ir

INTRODUCTION

Pixelated crystals in medical imaging have an important role to enhance spatial resolution of planar detection. They are arranged regularly in a detection system but the generated signals from the readout electronics behind the crystal impose irregularities in the shape of final image. These image irregularities should be corrected before further processes on the image. The correction is performed by mapping the image pixels to crystal pixels [1-4].

In many gamma detectors in high resolution nuclear medicine imaging systems (SPECT and PET), pixelated scintillation crystals are used [5, 6]. Due to the errors in the detection system and the noise, there is always an uncertainty in estimating the incidence position of the gamma photons relative to the true position. Given such uncertainty, a positioning calibration is necessary in all nuclear medicine imaging modalities. When pixelated crystals are used, by irradiating the crystal with a uniform emission of gamma photons, an image including some hot points (peaks) each corresponding to a pixel is resulted; such an image is called "flood image." The flood image is arranged in a larger matrix relative to the array size of the pixelated crystal [7].

Earlier works use the simplest method by manually locating the pixel peaks and assigning them to the crystal pixels [2]. The first step in the position calibration is to determine the position of the peaks, precisely. The process of finding the position of the peaks is called "peak detection". Following the peak detection, a mapping process is performed regarding the position of the peaks and the known position of the pixels. Since the manual procedure is time consuming when the number of crystals is high for example in PET scanners, the automatic methods have been developed using Gaussian mixture models [8-10] and neural network implementation [11, 12]. However, they do not have appropriate result in the case of noisy images in nuclear medicine imaging. In this work a novel approach for the peak detection algorithm in the presence of noise and distortion is proposed. At the beginning, a Gaussian filter is applied on the image. Two stages of local peak detection are then performed by applying two different window widths to locate the peaks. After detecting the peak positions and assigning them to the crystal pixels, the algorithm uses thin-plate spline [13] to restore the distorted image to the regular matrix and maps all other image pixels to the crystal pixels. This algorithm was initially created to function as part of the calibration software for a new small animal PET detector block [4, 14].

METHODS

In the pixelated crystals, the first step in the positioning calibration is to irradiate the crystal by a uniform source of activity. The flood image is acquired from 24×24 array of LYSO:Ce crystals with 2×2×10 mm^3 pixel size and 0.05 mm $BaSO_4$ reflector which results 2.1 mm pixel pitch. The crystal array is showed in Figure 1. This leads to a dotted image which is called the flood-field (or flood) image in the 512×512 matrix size. Two sample flood images obtained from a 24×24 crystal array coupled to 12×12 SiPM array is demonstrated in Figure 2. Each dot represents the response of a system to the interactions which occurred in the single crystal element (pixel). However, the flood image with large matrix size cannot be used in its raw structure for the aim of tomographic imaging, and should be converted to a digitized $m \times n$ image, where m and n are the number of pixels in each dimension of the crystal. Since the 2 mm light guide results more regular shape in the flood image, to better evaluate the algorithm performance we demonstrated the 1 mm light guide calibration results in this work. In the imaging purpose, 2 mm light guide is used in the detector design.

The next step is to generate a look up table (LUT) mapping the position (X and Y) of each point in the flood-field image to the crystal pixels. The table can be generated using the known physical position of the crystal pixels and the peak position of the response of the corresponding pixels in the flood-field image. Since the flood-field image in gamma detectors may not have high-quality and instead, the response of each pixel is a blurred point in a noisy background, determining the peak position of each blurred response is mandatory which is later used as the position of the response of the elements. The flow diagram of the process for generating LUT to calibrate the estimated position is shown in the Figure 3.

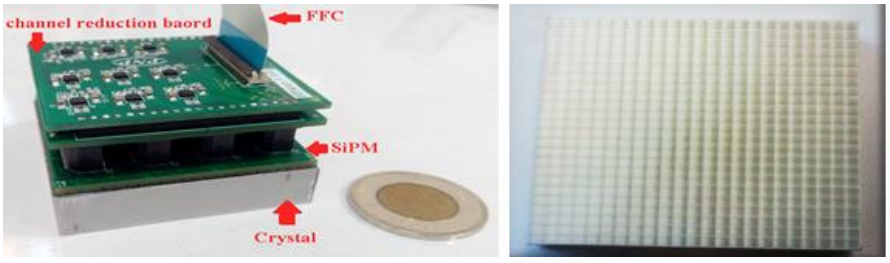

Fig 1. The LYSO crystal array (right) and the frontend electronic (left) to readout the position of the gamma interaction.

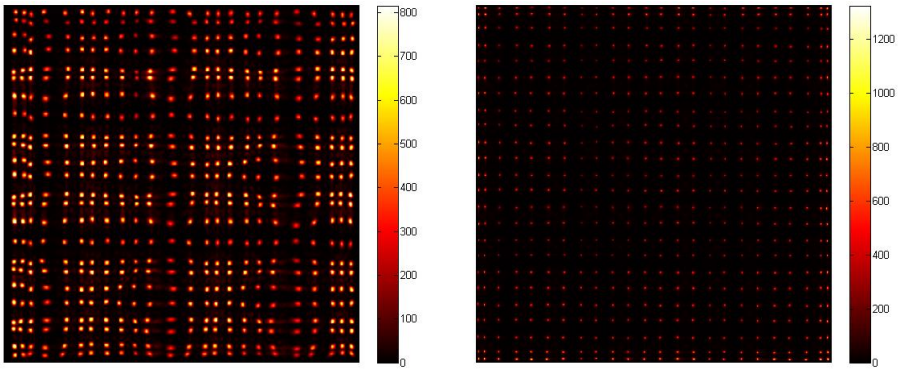

Fig 2. The crystal flood image with 1 mm (left) and 2 mm (right) light guides with 4 M counts acquired by the lutetium intrinsic activity in 10 min.

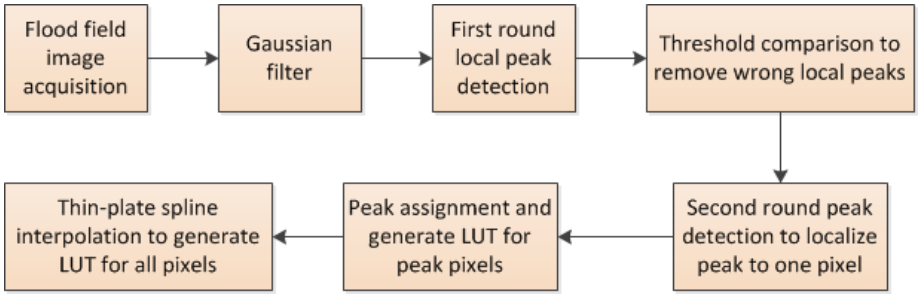

Fig 3. The 2D position calibration flow for the gamma imaging detectors.

In the first step of the algorithm, the flood-field image is filtered (convolved) by a 2D digital Gaussian function (F) with the pre-determined kernel size and the standard deviation (σ). The filter is defined so that, the sum of all its elements is '1' in order to be count value conservative (i.e. no influence on the total number of counts in the image after convolution). The process can be formulated as:

$$I_f = I * F \qquad (1)$$

Where $\boldsymbol{I}$ and $\boldsymbol{I_f}$ are the flood-field image and the filtered image, respectively. The kernel size should be large enough to include enough portion of the Gaussian curve regarding to its standard deviation. However, it should be also noted that a larger kernel size causes more computational burden.

In the next step, a 2D window with the size of ω_1 is moved on the matrix $\boldsymbol{I_f}$ and the local peaks in each window step are determined. Matrix P is defined as a matrix with the same size of matrix I (and I_f) which all of its elements is set to zero. Local peak is defined when a pixel value is greater than the majority of pixels in the window. In a given window, C_1 is defined as:

$$C_1 = {\omega_1}^2 - \alpha, \quad (1 \le \alpha \le {\omega_1}^2) \qquad (2)$$

where α is a parameter of the algorithm which represents a portion of the pixels placed inside the window ω_1, and $\omega_1$is the window width at the first local peak detection. When a pixel value is greater than the value of at least C_1 pixels in the window (pixels in the ω_1 window) then its value will be registered in the matrix P at its corresponding position in the matrix I_f. To remove wrong local peaks, a threshold is defined to compare local peak values. This threshold level can be defined according the all found peak values but, it may remove a true peak if the sensitivity of according crystal pixel is much lower than the other crystals. This usually happens at the crystal array edges. Therefore we defined the threshold level according the found peak values in a fixed neighbor window. This window width is determined so it should contain at least one true peak. The mean value of the non-zero elements in window of matrix P is calculated as:

$$mean = \left(\frac{sum_{nonzero}}{n_{nonzero}}\right) \qquad (3)$$

where $sum_{nonzero}$ is the sum of all non-zero elements in the window and $n_{nonzero}$ is the number of non-zero elements in the window. If the value of each non-zero element is smaller than *threshold*×*mean*, the element is set to zero. '*Threshold*' is a parameter of the algorithm in the range of 0 and 1.

In the next step, the second iteration for local peak detection is repeated by considering matrix P *as* the input matrix.

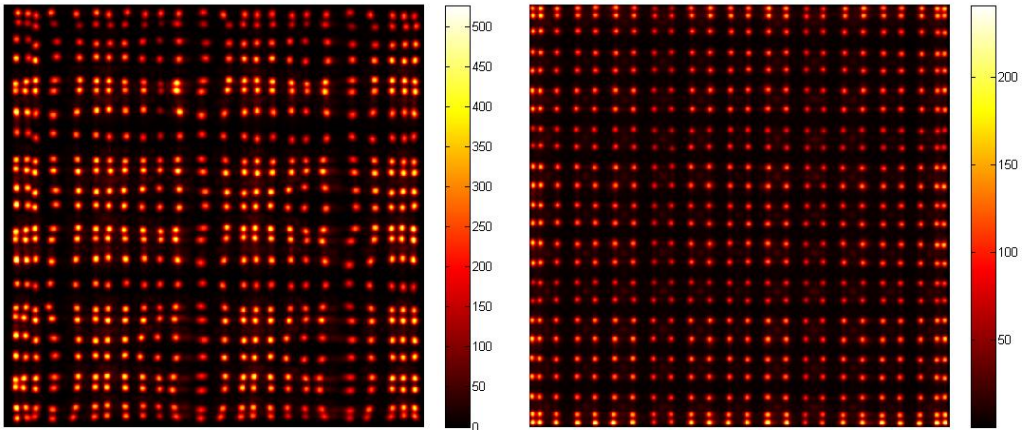

Fig 4. Applying Gaussian filter on the flood images with 15 pixel kernel and $\sigma = 2$.

A new window with the size of 3 (the adjacent pixels) for local peak search is used, and the resultant matrix is called P_2. Same as the first step, if the value of the pixel is greater than the all other pixels in the window, the pixel will be considered as a true peak. In this iteration also, the mean value is calculated by (Eq.3) and the window threshold is applied to eliminate false peaks in the image. The matrix P_2 that now should have exact number of non-zero elements equal to the crystal pixel numbers, is used as the input for the next step of the algorithm.

In this step the detected peaks will be assigned to the crystal pixels. We assume a 'band' in P_2 as a subset of rows where the number of peaks in the band is equal to the number of physical pixels in each crystal row and $n_{Band\ Peaks}$, $Band_L$, and $Band_U$ as the number of peaks in the band, the lowest row of the band, and the highest row of the band, respectively. The initial value of these parameters is set as:

$$n_{Band\ Peaks} = 0,$$
$$Band_L = 0,$$
$$Band_U = 1,$$

The algorithm will increment $Band_U$ and calculate $n_{Band\ Peaks}$ until, $n_{Band\ Peaks}$ get equal to the number of pixels in a crystal row. The image peak locations in the band will be assigned to the crystal pixels according the column number. To generate and assign the next band, $Band_L$ is set to $Band_U + 1$, then the above procedure is performed for the new band. In this way, the order of peaks corresponding to the order of pixels in the crystal can be obtained, automatically.

In order to decrease the noise effect in positioning the peaks, the center of mass method is applied for each peak prior to generating LUT. A square neighborhood with the size of ω_{COM} (in each dimension) is defined around each peak obtained from the previous stage. Then, using the neighbor's values in the matrix I (the initial image matrix), the center of mass is calculated and is considered as the position of the peak. It should be noted that the values mentioned through the description of the method, as the parameters of the algorithm, should be determined once for every system regarding the different inherent parameters of the system.

After all the desired peaks in the image successfully located and numbered respectively, the thin-plate spline method which is described in detail in [13] is used to map the distorted grid of pixels in the image to a regular shape matrix. The method uses 24×24 fixed points in the image and their certain final location (crystal pixel number), and interpolates other image pixels by solving the mapping equations for the unknown points. The generated matrix will be used as the LUT for position correction.

RESULTS

The detector set up has been tested with two different light guides with 1 mm and 2 mm thicknesses. We used intrinsic lutetium activity to generate flood image instead of irradiating by an external source, and the results are shown in Figure 2. For the detection of the optical photons we used ARRAYC-30035-144P from SensL (Cork, Ireland) which is 12×12 array of SiPM pixels coupled to the crystal array and light guide. The active pixel size of SiPM is 3×3 mm^2 and the size of the array is 50.2×50.2 mm^2 with the pixel pitch 4.2x4.2 mm^2. The signal of SiPM pixels are read by the developed hardware with the scrambled cross wire method. The detector block is detailed in [4]. Both images have been tested with the presented method for automatic position calibration.

The acquired images are arranged in 512×512 matrix and the Gaussian filter is convolved with the 2D images by 15 pixel kernel size and $\sigma = 2$. The result of filter convolution is shown in the Figure 4.

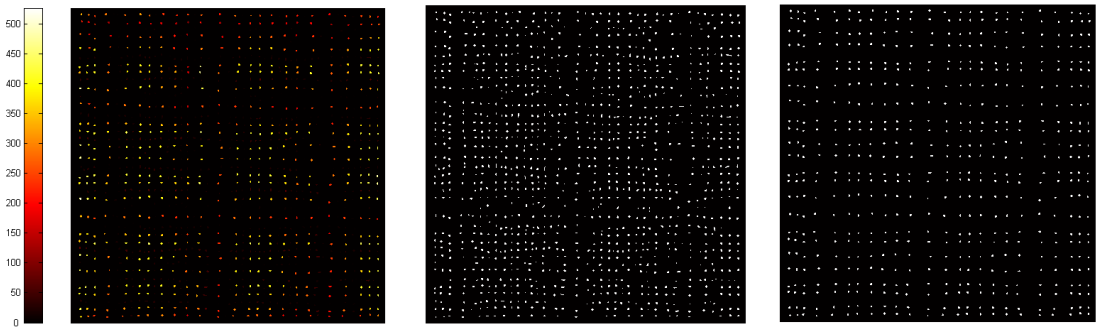

Fig 5. The first window on the peak detection algorithm is performed with 7×7 pixels and the resulting image shows the detected main peaks (left image). By setting all non-zero values to 1, the wrong peaks in the image with relatively small values are visible (middle image). The window threshold method removes wrong peaks having smaller value rather than a portion of the average near peak values (right image).

The first window (ω_1) is set 7×7 with $C_1 = 41$ out of total 49 pixels in the window. The local peak positions were detected and are shown in Figure 5 (left). The local peaks with relatively small values are also detected which can be seen in Figure 5 (middle) by setting all non-zero values to 1. The use of the threshold level for peak value over the window removes the wrong peak locations Figure 5 (right).

The second step procedure is same as first round with the window of 3×3 and $C_1 = 8$. This step removes all non-zero values except the peak locations (localize peak location to one pixel) which is required for peak assignment routine. The Figure 6 shows the peak assignment routine, which in each step assigns detected peaks in a band to the crystal pixels in a row.

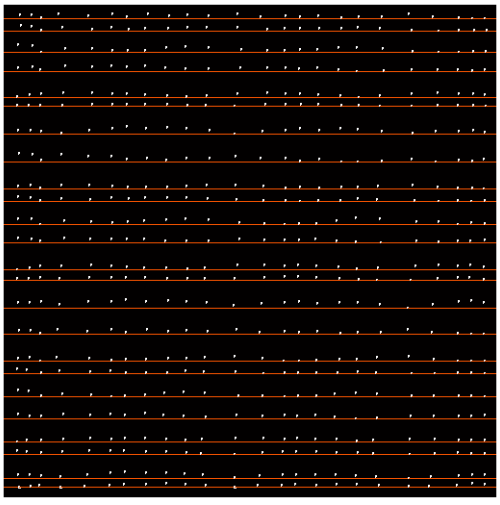

Fig 6. Band detection and separation method for assigning image peaks in a band to the crystal pixels in a row

Given the known image peaks and the corresponding crystal pixels, the algorithm produces required equations for the thin-plate spline interpolation [13]. By solving the equations, the image will be divided to $m \times n$ regions according to m and n crystal pixels in each dimension (Figure 7, left), then the image pixels in each region will be mapped to the corresponding crystal pixel (Figure 7, right).

The total time for the calibration routine after preparation of the flood image until creation of the correction look-up table in the core-i5 processor is measured 75 s. Total 10 blocks of the same detector architecture and 2 mm light guide are calibrated using the presented algorithm. By applying proper parameters for one detector, the method calibrated all other ten block in the scanner without error.

DISCUSSION

We designed a method to use on flood image of gamma camera pixelated crystal. The first peak detection step using moving window is designed to detect local peaks. The window width is defined so that it usually contains one true peak in each position. The definition of threshold level in next step is important to correctly remove the unwanted peak locations. If we use the all peak values for definition of the threshold some of wrong peaks in the middle of two peaks with large values will remain all some border line crystal pixel's peak location will be lost due to the small value. By using window based threshold definition the local peaks will be compared with true neighbor peaks and they will not be lost. The last peak detection shrinks the peak positions to one pixel.

Finally the band definition will arrange distorted rows of peak positions to crystal regular shape. If the distortion becomes too severe so that for example peak position at the edges of one row (peak 'a' in Figure 8) locates higher than some peak positions at the center of the next row (peak 'b' in Figure 8), this algorithm fails to arrange peak positions correctly.

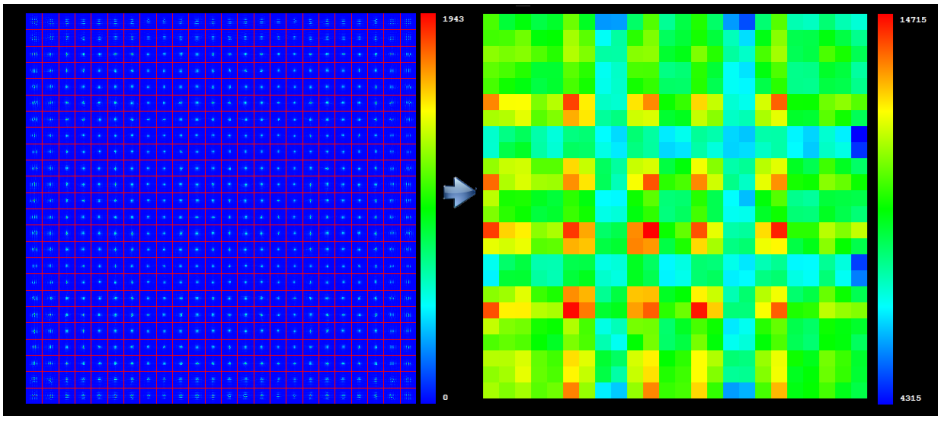

Fig 7. The thin-plate spline interpolation method divides detector image according the known detected peaks in the image and the crystal pixels and interpolates other image pixels (left). The flood-field image will be corrected by mapping the image pixels to the corresponding crystal pixel position (right).

This happens usually in the severe cushion effect when there is shrinkage at the center or the corners of the image. In this situation, a correction factor should be applied to slightly compensate the cushion effect prior the automatic peak detection algorithm.

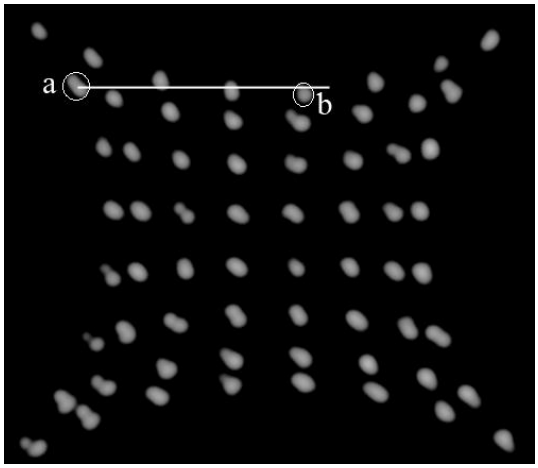

Fig 8. Severe cushion effect which fails peak assignment algorithm.

Manual methods are also used in such cases where a user determines the peak position. However, such methods are highly dependent on the user's skill. In addition, they suffer from not being reproducible, and time consuming when there are many detector blocks to be calibrated and each have too many crystal pixels. A precise automatic algorithm can be beneficial in position calibration for nuclear medicine imaging modalities. Although there are various general peak detection methods, they cannot act precisely enough in the presence of noise and disturbance in nuclear medicine imaging.

For the future work, to compare the noise robustness and errors in the presented algorithm and the other automatic algorithms [8, 9] further evaluation of the methods using different algorithms are warranted.

CONCLUSION

An algorithm is proposed for automatic 2D peak detection and position correction of nuclear medicine images. The peak detection is the first stage in position calibration in PET or linearity calibration in SPECT. The algorithm composed of some successive steps including a 2D Gaussian filtering and two local peak positioning steps. The advantage of this method over the conventional peak detection methods is its automatic performance after setting up some initial parameters along with the ability to perform on noisy data.

Acknowledgments

This work was partially funded by Tehran University of Medical Sciences under Grant No. 34450.

REFERENCES

1. Dahlbom M, Hoffman EJ. An evaluation of a two-dimensional array detector for high resolution PET. IEEE Trans Med Imaging. 1988;7(4):264-72.
2. Akbarzadeh A, Saba V, Ay MR. New approach for calibration of pixelated scintillation detectors of intraoperative gamma cameras. Iran J Nucl Med. 2017;25(1):34-42.
3. Kaviani S, Zeraatkar N, Sajedi S, Akbarzadeh A, Gorjizadeh N, Farahani MH, Teimourian B, Ghafarian P, Sabet H, Ay MR. Design and development of a dedicated portable gamma camera system for intra-operative imaging. Phys Med. 2016 Jul;32(7):889-97.
4. Sajedi S, Zeraatkar N, Taheri M, Kaviani S, Khanmohammadi H, Sarkar S, Sabet H, Ay MR. A Generic, scalable, and cost-effective detector front-end block for PET. IEEE Nucl Sci Symp Med Imaging Conf. (NSS/MIC), 2017.

5. Levin CS, Zaidi H. Current trends in preclinical PET system design. PET Clin. 2007 Apr;2(2):125-60.

6. Madsen MT. Recent advances in SPECT imaging. J Nucl Med. 2007 Apr;48(4):661-73.

7. Flower MA. Webb's physics of medical imaging. 2nd ed. CRC Press; 2012.

8. Schellenberg G, Stortz G, Goertzen AL. An algorithm for automatic crystal identification in pixelated scintillation detectors using thin plate splines and Gaussian mixture models. Phys Med Biol. 2016 Feb 7;61(3):N90-N101.

9. Stonger KA, Johnson MT, Optimal calibration of PET crystal position maps using Gaussian mixture models. IEEE Trans Nucl Sci. 2004;51(1):85-90.

10. Yoshida E, Kimura Y, Kitamura K, Murayama H. Calibration procedure for a DOI detector of high resolution PET through a Gaussian mixture model. IEEE Trans Nucl Sci. 2004;51(5):2543-2549.

11. Hu D, Atkins BE, Lenox MW, Castleberry B, Siegel SB. A neural network based algorithm for building crystal look-up table of PET block detector. IEEE Nucl Sci Symp Conf Record, 2006.

12. Hu D, Gremillion T. Verification of neural network based algorithm for crystal identification of PET block detector. IEEE Nucl Sci Symp Conf Record, 2007.

13. Bookstein FL. Principal warps: Thin-plate splines and the decomposition of deformations. IEEE Trans Pattern Anal Mach Intell. 1989;11(6):567-585.

14. Zeraatkar N, Sajedi S, Kaviani S, Taheri M, Khanmohammadi H, Sarkar S, Ay MR. Development of a preclinical PET system based on pixelated LYSO crystals and SiPM. IEEE Nucl Sci Symp Med Imaging Conf. (NSS/MIC), 2017.